

Optical Spectroscopic Monitoring of Pre-Main Sequence Stars: the UXOr Sub-Sample.

I. Mendigutía, B. Montesinos, C. Eiroa, and A. Mora

Abstract The EXPORT consortium carried out in 1998–1999 photo-polarimetric and spectroscopic monitoring over 74 Pre-Main Sequence (PMS) and MS stars with infrared excesses, 43 of them showing the $H\alpha$ line in emission. We have measured the equivalent widths (EWs) of the $H\alpha$, [OI]6300, HeI5876 and NaID lines in 370 intermediate resolution optical spectra, obtained along four different observing campaigns, of those 43 objects. In this contribution we focus on the simultaneous spectroscopic and photometric behaviour of 12 UX-Ori type variable stars included in the sample. The main results indicate that the $EW(H\alpha)$ - V correlation is a main feature of UXOrs. This correlation is also found in the [OI]6300 line in most of the objects. The variability in $EW(HeI5876)$ -but not in the flux (F) in several cases- does not depend on the V -behaviour, as well as the complex patterns displayed in the NaID lines. We interpret these results according to the dusty obscuration effect generated by the disks surrounding these stars, and propose that different accretion mechanisms could operate in different objects, depending on their $F(HeI5876)$ - V behaviour.

Ignacio Mendigutía

Laboratorio de Astrofísica Espacial y Física Fundamental (CAB/LAEFF/INTA), European Space Astronomy Centre, PO Box 78, E-28691 Villanueva de la Cañada, Madrid, Spain, e-mail: Ignacio.Mendigutia@laeff.inta.es

Benjamín Montesinos

Laboratorio de Astrofísica Espacial y Física Fundamental (CAB/LAEFF/INTA)

Carlos Eiroa

Universidad Autónoma de Madrid (UAM)

Alcione Mora

Universidad Autónoma de Madrid (UAM)

1 Introduction

One main feature of PMS objects is the photometric and spectroscopic variability, usually connected to the presence of circumstellar (CS) disks. The UXOr phenomenon was firstly characterized according to the polarization increase and reddening observed when some PMS stars fade in their V-magnitude [15]. Subsequent works related to the spectroscopic behaviour of this type of objects noted that UXOr stars display an enhancement in the strength of different spectroscopic lines, mainly $H\alpha$, as the brightness of the central object decreases [12, 13, 27]. These facts have been explained according to the coronographic effect produced by part of the dusty material harboured in their CS disks [10], which might be oriented almost edge-on [11, 24].

Broadly speaking, the behaviour of PMS stars in several spectroscopic lines, such as $H\alpha$, [OI]6300, HeI5876 or NaID, clearly differ from that observed in MS objects. These lines probe different parts of the disks and are originated by different physical mechanisms. The $H\alpha$ emission line is the most prominent spectral feature in all intermediate-mass PMS objects and in the so-called Classical T Tauri (CTT) stars, and it is related to magnetospheric accretion/wind processes [16]. The origin and the physical information provided by the HeI5876 line in PMS objects have been also associated to accretion phenomena, since it might be generated in the very inner region of the CS environment where the accreting gas hits the stellar surface at $T > 15000$ K [30, 13]. On the other hand, the [OI]6300 line, observed in emission in many PMS stars, must be generated in the lower density parts of the CS disks, usually associated to disk winds and jets [4, 3]. Finally, although interstellar clouds in the line of sight make it difficult to study the NaI resonance doublet in CS disks [26], significative variations in these lines are associated to complex gas motions around PMS stars [22, 23], which could be connected with both magnetospheric accretion and star-grazing planetesimal bodies [29, 13].

In order to characterize the spectroscopic variability of PMS objects, we have studied 370 intermediate resolution spectra of 43 PMS stars showing the $H\alpha$ line in emission, obtained from the monitoring carried out by the EXPORT consortium [9]. In this contribution we summarize the results derived from the study of the simultaneous evolution of the EWs and Fs in the $H\alpha$, [OI]6300, HeI5876 and NaID lines and the V-magnitudes of 12 UX-Ori type stars included in the sample¹. In Sect. 2 we describe the sample and spectra studied. The results obtained from the crossmatching between the spectroscopic and the photometric values of the UXOr sub-sample are briefly described and commented in Sect. 3.

¹ A deeper study devoted to the optical spectroscopic variability of the whole sample and the complete results related to the UXOr-subsample will be published in two forthcoming papers (Mendigutía et al. 2009, in prep.)

2 Observations and characterization of the sample

370 intermediate resolution spectra obtained from the monitoring of 43 PMS objects have been characterized. In order to study only the non-photospheric contribution, additional spectra of 28 spectroscopic standard (MS) stars of similar spectral types were rotationally broadened and subtracted from the target ones. Each final non-photospheric spectrum was normalized to unity. All spectra were taken by the EXPORT consortium [9, 21] over four observing campaigns of several days each (14–17 May, 28–31 July, 24–28 October 1998, and 28–31 January 1999). The spectra cover the 5800–6700 Å wavelength range, and were obtained with the 2.5 m Isaac Newton Telescope (INT) at Roque de los Muchachos observatory (La Palma, Canary Islands) with a typical spectral resolution of ~ 5500 . The observations and data reduction are described in detail in [21].

The 43 PMS objects of the sample display the $H\alpha$ line in emission. They are mainly intermediate-mass PMS stars since only four are CTTs. The age of the stars cover the 0–17 Myr range [17, 20]. The ratio between the infrared excess and the stellar flux (F_{ir}/F_*), indicative of the optical depth of the CS disk, range between 0.006 and 74.82 [19]. From the EXPORT observations, 13 out of the 43 objects (see table 1) were classified as UXOrs by [25]. Some others have also been classified in a similar way [28], although they did not display the UXOr phenomenon in the EXPORT campaigns and we will not consider them in the results of the present work.

Table 1 Stars studied in the present work. All showed the UXOr phenomenon in the EXPORT campaigns (Oudmaijer et al. 2001).

Star	Spectral Type ¹	$(F_{\text{ir}}/F_*)^2$	Age (Myr) ^(3; 4)	Vmin; Vmax ⁵	Vmin; Vmax ⁶
BM And	K5 Ve	1.398	...; ...	12.40; 14.60	12.27; 13.34
VX Cas	A0 Vep	...	1.12; $6.4^{+4.0}_{-1.5}$	10.70; 13.30	11.39; 12.95
BH Cep	F5 IIIev	0.442	8.21; ...	11.50; 12.70	11.23; 12.18
VY Mon	A5 Vep	74.82	< 0.01; ...	13.70; 17.40	...; ...
KK Oph	A8 Vev	34.53	3.93; ...	11.90; 12.70	12.06; 12.67
BF Ori	A2 IVev	0.655	2.72; $3.2^{+1.3}_{-0.9}$	9.80; 13.40	9.65; 9.79
HK Ori	G1 Ve	0.96	0.96; ...	11.10; 13.30	11.44; 11.79
RY Ori	F6 Vev	1.202	1.77; ...	10.80; 13.90	11.36; 12.34
DK Tau	K5 Ve	1.006	...; ...	11.90; 15.10	12.08; 12.89
RR Tau	A0 IVev	3.164	0.13; $0.4^{+0.3}_{-0.2}$	10.20; 14.20	10.92; 11.46
RY Tau	F8 IIIev	4.734	...; ...	9.30; 12.30	10.47; 10.67
WW Vul	A2 IVe	0.902	...; $3.7^{+3.7}_{-1.7}$	10.90; 12.60	10.64; 11.03
LkHa 234	B5 Vev	5.728	< 0.01; ...	11.9	12.73; 12.96

¹Mora et al. (2001), ²Merín (2004), ³Manoj et al. 2006, ⁴Montesinos et al. 2008, ⁵SIMBAD (<http://simbad.u-strasbg.fr>), ⁶V-magnitudes for which there are simultaneous spectroscopic measurements from the EXPORT campaigns.

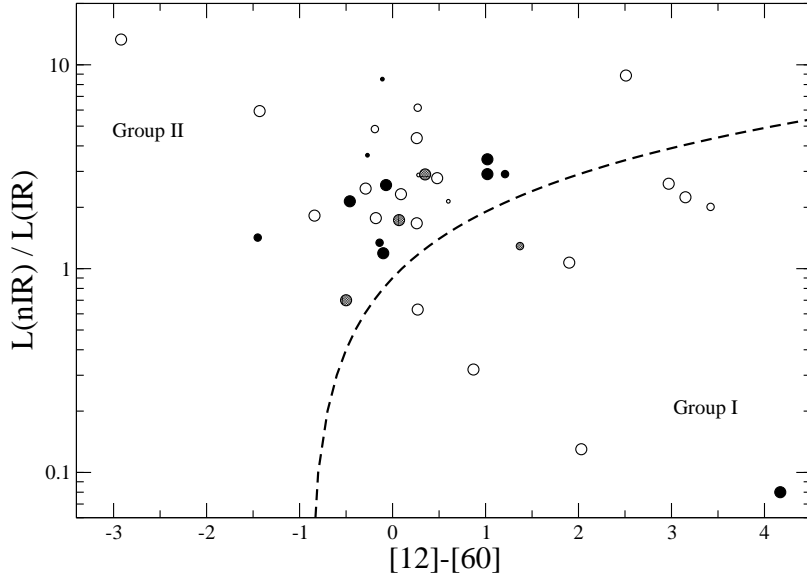


Fig. 1 Ratio between near-infrared and total infrared luminosity vs IRAS 12-60 colour for most of the stars of the sample. See the text for references on this diagram. CTTs, ETTs and HAeBes are represented by dots of increasing sizes. Black dots indicate the UXOrs from the EXPORT campaigns (LkHa 234 is located at the right-bottom side of the graph). Grey dots indicate well-known UXOrs [28] not displaying the phenomenon in the EXPORT campaigns.

In order to further characterize the sample, we have located most of the objects in a diagram (see Fig. 1) firstly derived by [31], and based in the SED classification scheme made by [18]. The distinction in this diagram between Group I and Group II sources has been associated to physical, geometrical and evolutionary differences of PMS stars [18, 6, 7, 8, 1, 2]. Only seven out of the 42 objects included in the sample do not have enough data for setting its position in Fig. 1. For the rest of the stars, the sample is clearly biased towards Group II since 27 stars belong to it, and only 9 are Group I sources. Despite of this, there exists a clear statistical connection between the UXOr phenomenon and Group II sources. As it can be seen from Fig. 1, all the UXOr-stars are (or are very close to be) Group II sources. The only clear exception is LkHa 234, one of the youngest known HBe stars [5]. The fact that this object is embedded in the IC 5134 nebula could explain its anomalous position in the diagram, since this is derived from IRAS measurements. Taking this into account, the latter results are in agreement with those obtained by [7], indicating that obscuration effects are probably not associated to the outer disk but to the inner, as also indicates the typical time-scales of the dimming observed in UXOr-stars.

The next Section is focused on the results derived by crossmatching simultaneous spectroscopic measurements and optical photometric values available for 12 stars displaying the UXOr phenomenon in the EXPORT campaigns.

3 Summary of results and discussion

The EW measurements of the 13 stars displaying the UXOr phenomenon in the EXPORT campaigns (see table 1) has been crossmatched with simultaneous (i.e, obtained in the same night) V-magnitudes obtained from [25]. In the case of VX Cas, V-magnitudes from [14] have also been used. The combination between the simultaneous EWs and V (or R) magnitudes has been used to derive the HeI5876 and NaID (or H α and [OI]6300) line fluxes. There is no simultaneous photometry in the case of VY Mon. The summary of the main results for the rest of the stars displayed in table 1 follows:

1. The EW(H α) increases as the brightness of the stars fades, independently of the V-ranges studied. Only DK Tau does not follow this correlation. The rest of the objects keep their F(H α) approximately constant with the only two exceptions of VX Cas (F(H α) and V anti-correlate) and RY Ori (F(H α) and V correlate). The stars showing the [OI]6300 line (8 out of the 12 stars studied) follow a similar correlation between EW([OI]6300) and the V-magnitude. Similarly, F([OI]6300) tends to remain constant in all these cases. These results are well in agreement with the coronographic effect exerted by a dusty screen located close to the inner rim of the disk. The enhancement of the EW is caused by the contrast between an almost constant line flux and the decrease of the continuum contribution.
2. The variability in the EW(HeI5876) is not correlated with the brightness variations. Regarding the behaviour of F(HeI5876), two groups can be considered. The stars belonging the first one (BM And, BF Ori, DK Tau, VX Cas and BH Cep) display a minimum value of F(HeI5876) at the maximum available V-value. In the second group, composed by the rest of the objects, the variations in F(HeI5876) are not correlated with the stellar brightness. Although a simultaneous monitoring in V and infrared spectral lines as Pa β or Br γ is necessary, the latter result would indicate that accretion rate variations do not seem to affect significantly the stellar brightness. A possible explanation for the differences between the two groups could be associated with the physical mechanism by which the objects accrete. Assuming that the HeI5876 line arises from the interface between the accreted material and the stellar surface [30], we would expect the flux of this line to decrease as the star fades in those objects for which the accreted material contacts the stellar surface at low latitudes, since UXOr-stars are supposed to be oriented roughly edge-on and the obscuring dusty screen intersecting the line of sight might be located in the plane of the CS disk. On the other hand, if accretion happens at high latitudes, the screen would not affect the measured F(HeI5876). Therefore it is worth to study the behaviour of UXOrs in this spectral line since it could give hints to understand how intermediate-mass PMS stars accrete -boundary layer or magnetospheric accretion-.
3. As it has been reported before (e.g. [27]), we also find complex patterns -i.e changes in the strength of the lines, changes from absorption to emission or appearance of transient absorption components- in the EWs of the NaID lines,

which could be related to the variations and dimming of the stellar brightness. Nevertheless, it should be noted that similar variations are observed in UXOr-stars at high brightness and when their V-magnitude remains almost constant. As an example, DK Tau, KK Oph, HK Ori, or RY Tau change their NaID profiles from absorption to emission in the narrow V-ranges indicated in table 1. In the case of BF Ori, the V-magnitude, observed along the same week, ranges only between 9.65 and 9.79, but the EW(NaID) changes by a factor ~ 5 (even higher than the factor ~ 4 observed in VX Cas, monitored in a wider range of its V-magnitude). These results indicate that gas blobs, not coupled with dust, usually intersect the line of sight without causing any variation in the observed stellar brightness.

References

1. Acke, B. & van den Ancker, M.E. 2004, A&A, 426, 15
2. Acke, B., van den Ancker, M.E., Dullemond, C.P., van Boekel, R., Waters, L.B.F.M. 2004, A&A, 422, 621A
3. Acke, B., van den Ancker, M.E., Dullemond, C.P. 2005, A&A, 436, 209
4. Corcoran, M. & Ray, T.P. 1997, A&A, 321, 189
5. Chakraborty, A., Ge, J., Mahadevan, S. 2004, ApJ, 606, L69
6. Dullemond, C.P. 2002, A&A, 395, 853
7. Dullemond, C.P., van den Ancker, M.E., Acke, B., van Boekel, R. 2003, ApJ, 594, L47
8. Dullemond, C.P. & Dominik, C. 2004, A&A, 417, 159
9. Eiroa, C. and 23 coauthors, 2000, ESASP, 451, 189
10. Grinin, V.P., Kiselev, N.N., Minikulov, N.Kh., Chernova, G.P. 1988, SvAL, 14, 219G
11. Grinin, V.P., Kiselev, N.N., Minikulov, N. KH., Chernova, G.P., Voshchinnikov, N. V., 1991, Ap&SS, 186, 283
12. Grinin, V.P., The, P.S., de Winter, D., Giampapa, M., Rostopchina, A.N., Tambovtseva, L.V., van den Ancker, M.E. 1994, A&A, 292, 165
13. Grinin, V.P., Kozlova, O.V., Natta, A., Ilyin, I., Tuominen, I., Rostopchina, A.N., Shakhovskoy, D.N. 2001, A&A, 379, 482
14. Grinin, V.P. et al. 2009 A&A. in prep.
15. Herbst, W., Herbst, D.K., Grossman, E.J., Weinstein, D., 1994, AJ, 108, 1906
16. Kurosawa, R., Harries, T.J., Symington, N.H. 2006, MNRAS, 370, 580
17. Manoj, P., Bhatt, H.C., Maheswar, G., Muneer, S. 2006, ApJ, 653, 657
18. Meeus, G., Waters, L.B.F.M., Bouwman, J., van den Ancker, M.E., Waelkens, C., Malfait, K. 2001, A&A, 365, 476
19. Merín, B. 2004, Phd thesis, Universidad Autónoma de Madrid
20. Montesinos, B., Eiroa, C., Merín, B., Mora, A. 2008, A&A, submitted.
21. Mora, A. and 21 coauthors, 2001, A&A, 378, 116
22. Mora, A. and 23 coauthors, 2002, A&A, 393, 259
23. Mora, A. and 24 coauthors, 2004, A&A, 419, 225
24. Natta, A., Grinin, V.P., Mannings, V., Ungerechts, H. 1997, ApJ, 491, 885
25. Oudmaijer, R.D. and 22 coauthors, 2001, A&A, 379, 564.
26. Redfield, S. 2007, ApJ, 656, L97
27. Rodgers, B., Wooden, D.H., Grinin, V., Shakhovsky, D., Natta, A. 2002, ApJ, 564, 405
28. Rodgers, B. 2003, ASPC, 287, 180
29. Sorelli, C., Grinin, V.P., Natta, A. 1996, A&A, 309, 155
30. Tambovtseva, L.V., Grinin, V.P., Kozlova, O.V. 1999, Astrophysics, 42, 1
31. van Boekel, R., Waters, L.B.F.M., Dominik, C., Bouwman, J., de Koter, A., Dullemond, C.P., Paresce, F. 2003, A&A, 400, L21-L24